Mechanism of Adenylate Kinase. Demonstration of a Functional Relationship between Aspartate 93 and Mg^{2+} by Site-Directed Mutagenesis and Proton, Phosphorus-31, and Magnesium-25 NMR†

Honggao Yan and Ming-Daw Tsai*

Department of Chemistry and Ohio State Biochemistry Program, The Ohio State University, Columbus, Ohio 43210

Received January 11, 1991; Revised Manuscript Received March 14, 1991

ABSTRACT: Earlier magnetic resonance studies suggested no direct interaction between Mg^{2+} ions and adenylate kinase (AK) in the AK·MgATP (adenosine 5′-triphosphate) complex. However, recent NMR studies concluded that the carboxylate of aspartate 119 accepts a hydrogen bond from a water ligand of the bound Mg^{2+} ion in the muscle AK·MgATP complex [Fry, D. C., Kuby, S. A., & Mildvan, A. S. (1985) *Biochemistry 24*, 4680–4694]. On the other hand, in the 2.6-Å crystal structure of the yeast AK·$MgAP_5A$ [P^1,P^5-bis(5′-adenosyl)pentaphosphate] complex, the Mg^{2+} ion is in proximity to aspartate 93 [Egner, U., Tomasselli, A. G., & Schulz, G. E. (1987) *J. Mol. Biol. 195*, 649–658]. Substitution of Asp-93 with alanine resulted in no change in dissociation constants, 4-fold increases in K_m, and a 650-fold decrease in k_{cat}. Notable changes have been observed in the chemical shifts of the aromatic protons of histidine 36 and a few other aromatic residues. However, the results of detailed analyses of the free enzymes and the AK·$MgAP_5A$ complexes by one- and two-dimensional NMR suggested that the changes are due to localized perturbations. Thus it is concluded that Asp-93 stabilizes the transition state by ca. 3.9 kcal/mol. The next question is *how*. Since proton NMR results indicated that binding of Mg^{2+} to the AK·AP_5A complex induces some changes in the proton NMR signals of WT but not those of D93A, the functional role of Asp-93 should be in binding to Mg^{2+}. We then asked whether disruption of the interaction between Mg^{2+} and Asp-93 affects the interaction between Mg^{2+} and the nucleotide at the active site of AK. Analysis by ^{31}P NMR suggested that Mg^{2+} orients the conformation of the polyphosphate chain of bound AP_5A in WT but not in D93A. These results raised the question of whether Mg^{2+} could bind to D93A·nucleotide complexes, which was then probed by ^{25}Mg NMR. The results suggest that Mg^{2+} does bind to the D93A·AP_5A complex, but possibly only weakly. The weaker affinity of Mg^{2+} was also confirmed by kinetic analysis. However, the low activity of D93A cannot be restored by higher concentrations of Mg^{2+} ions. Thus Asp-93 plays critical roles in the binding and function of Mg^{2+} ions during the catalysis by AK. Substitution of Asp-93 with alanine also lowered the pK_a of His-36, which supports the proximity between Asp-93 and His-36. However, disruption of the interaction between Asp-93 and His-36 did not affect the conformational stability of the enzyme.

Although Mg^{2+} is required in the catalysis by adenylate kinase (AK),[1,2] the specific roles of Mg^{2+} and its interaction with the enzyme have not been established. Early magnetic relaxation studies have led to the classification of the enzymes requiring metal ions in catalysis into three types of coordination schemes: substrate bridge (E–S–M), metal bridge (E–M–S or $\overline{\text{E–M–S}}$), and enzyme bridge (S–E–M) (Mildvan & Cohn, 1970). Muscle AK was classified in the first category since there was no evidence for direct binding of Mg^{2+} to AK (Mildvan & Cohn, 1970; Mildvan, 1979; and references therein). However, the metal ion has been suggested to be close to His-36 on the basis of paramagnetic relaxation effects between the C2-H of His-36 and MnATP (McDonald et al., 1975) or CrATP (Smith & Mildvan, 1982). Later an aspartate residue has been suggested to be interacting with Mg^{2+}, directly or indirectly, on the basis of structural studies: in the "NMR model" proposed by Mildvan and co-workers, Asp-119 has been suggested to accept an H-bond from a water ligand of the bound Mg^{2+} ion in the muscle AK·MgATP complex (Fry et al., 1985; Mildvan & Fry, 1987); in the 2.6-Å crystal structure of the yeast AK·$MgAP_5A$ complex, Asp-93 has been shown to be in proximity to the Mg^{2+} ion, but it was unclear whether Mg^{2+} binds directly to the carboxyl group or via one or more water molecules (Egner et al., 1987; Dreusicke et al., 1988).

It has been shown that substitution of Asp-119 with an asparagine residue resulted in little perturbations in the kinetic parameters (Kim et al., 1990). This result disfavors the NMR

† This work was supported by a grant from National Science Foundation (DMB-8904727). This study made use of a Bruker AM-500 NMR spectrometer at the Ohio State University funded by NIH Grant RR01458 and the National Magnetic Resonance Facility at Madison supported by NIH Grants RR02301 and RR02781 and NSF Grant DMB-8415048. This is paper 9 in the series "Mechanism of Adenylate Kinase". For paper 8, see Yan et al. (1990b).

[1] Abbreviations: ADP, adenosine 5′-diphosphate; AK, adenylate kinase; AMP, adenosine 5′-monophosphate; AP_5A, P^1,P^5-bis(5′-adenosyl)pentaphosphate; ATP, adenosine 5′-triphosphate; 1D, one-dimensional; 2D, two-dimensional; DTT, dithiothreitol; EDTA, ethylenediaminetetraacetate; FID, free induction decay; GDP, guanosine 5′-diphosphate; GTP, guanosine 5′-triphosphate; NOE, nuclear Overhauser effect; NOESY, nuclear Overhauser enhanced spectroscopy; PAGE, polyacrylamide gel electrophoresis. SDS, sodium dodecyl sulfate; Tris, 2-amino-2-(hydroxymethyl)-1,3-propanediol; WT, wild-type.

[2] All of the muscle AKs are type-1 AK, with M_r 21 700, and are >80% homologous (Kishi et al., 1986). Other types of AK have different sizes and are less homologous (Schulz, 1987). Unless otherwise specified, the numbering system used in this paper is the conventional system for AK1. Although chicken muscle AK (cAK) has one additional residue near the N-terminal (Kishi et al., 1986), the Met-1 residue is absent in the cAK expressed in *E. coli* (Tanizawa et al., 1987). This makes numbering of cAK consistent with other AK1.

0006-2960/91/0430-5539$02.50/0

model but does not disprove it since asparagine can also accept an H-bond. The results of other site-directed mutagenesis studies also concluded that the NMR model requires serious revisions (Tian et al., 1988, 1990; Yan et al., 1990a,b). In this paper we report that substitution of Asp-93 by alanine resulted in a significant decrease in k_{cat} and in the inability of Mg^{2+} to orient the phosphate groups of bound $MgAP_5A$. Our system is chicken muscle AK[2] overproduced in *Escherichia coli* (Kishi et al., 1986; Tanizawa et al., 1987). The results are consistent with the X-ray structure of the yeast AK·$MgAP_5A$ complex and suggest that Asp-93 plays critical roles in the catalytic function of Mg^{2+} during the catalysis by AK.

Materials and Methods

Materials. The *E. coli* expression system for chicken AK was kindly provided by Dr. Nakazawa (Tanizawa et al., 1987). The oligonucleotide used for the construction of D93A AK, TTCCTCATTGCCGGCTACCCT, was obtained from the Biochemical Instrument Center of The Ohio State University. Mutagenesis and DNA sequencing kits were purchased from United States Biochemicals and Amersham, respectively. Reagents and coupling enzymes for kinetics were obtained from Sigma. Perdeuterated Tris was purchased from MSD Isotopes. ^{25}MgO (98 atom % ^{25}Mg) was obtained from Oak Ridge National Laboratory, and a stock solution of 0.25 M $^{25}Mg^{2+}$ was prepared by dissolving the oxide in perchloric acid followed by adjustment to pH 7 with NaOH and determination of the exact concentration by atomic absorption.

Site-Specific Mutagenesis and Purification of the Mutant Enzyme. The D93A mutant enzyme was constructed by the phosphorothioate analogue method of Taylor et al. (1985a,b) with an Amersham mutagenesis kit. Since the mutation efficiency was very high, the mutant was selected by DNA sequencing according to Sanger's dideoxy method using a DNA sequencing kit from United States Biochemicals. The mutant enzyme was purified and assayed essentially as described by Tian et al. (1988), except that a 50–300 mM linear NaCl gradient was used for eluting the phosphocellulose column. The purity of each preparation was checked by SDS–PAGE with silver staining on a PhastSystem.

Steady-State Kinetics. The kinetic experiments were carried out at 30 °C and pH 8.0 by measuring ADP formation with pyruvate kinase/lactic dehydrogenase as the coupling system (Rhoads & Lowenstein, 1968). The details have been described previously (Tian et al., 1988). The kinetic parameters were obtained by varying both MgATP and AMP concentrations and the data analyzed according to the equation of Cleland (1986). The K and K_i values (Michaelis and dissociation constants, respectively) obtained from such analysis are close to the K_m values (measured by saturating one substrate) and the K_d values (determined by titration studies with NMR), respectively (Sanders et al., 1989; Tian et al., 1990).

^1H NMR Methods. All ^1H NMR experiments were performed on Bruker AM-500 spectrometers. One- and two-dimensional proton NMR experiments were obtained at 25 °C, pH 7.8, as described previously (Yan et al., 1990b). For pH titration experiments, the pH was adjusted by addition of ^2HCl and NaO^2H, and all pH measurements were made at room temperature. The pK_as of histidine residues were obtained by nonlinear least-squares fitting of the chemical shifts of C2-H resonances as a function of pH according to a modified form of the Hill equation (Markley, 1974), with the Hill coefficient held at 1. It should be noted that the pH values were direct pH meter readings, and the pK_as obtained have not been corrected for the deuterium isotope effect.

Table I: Comparison of Kinetic, Binding, and Conformational Properties between WT and D93A[a]

parameter	unit	WT	D93A
Steady-State Kinetics			
k_{cat}	(s^{-1})	650	1
$K_{(MgATP)}$	(mM)	0.042	0.16
$K_{(AMP)}$	(mM)	0.098	0.47
$k_{cat}/K_{(MgATP)}$	(s^{-1} M^{-1})	1.55×10^7	6×10^3
$k_{cat}/K_{(AMP)}$	(s^{-1} M^{-1})	0.66×10^7	2×10^3
$K_{i(MgATP)}$	(mM)	0.16	0.11
$K_{i(AMP)}$	(mM)	0.37	0.33
Titration Experiments with NMR			
$K_{d(ATP)}$	(mM)	0.044	0.12
$K_{d(MgATP)}$	(mM)	0.17	0.37
$K_{d(AMP)}$	(mM)	0.50	0.25
Conformational Stability[b]			
$\Delta G_d^{H_2O}$	(kcal/mol)	4.5	4.0
m	(kcal/mol M)	5.7	5.6
Chemical Shifts of Bound AP_5A[c]			
H_2, with Mg^{2+}		8.98(I), 8.32(II)	8.99(I), 8.31(II)
no Mg^{2+}		8.92(I), 8.29(II)	8.99(I), 8.31(II)
H_8, with Mg^{2+}		8.47(I), 8.40(II)	8.65(I), 8.45(II)
no Mg^{2+}		8.50(I), 8.43(II)	8.65(I), *d*
$H_{1'}$, with Mg^{2+}		6.07(II), 5.93(I)	6.06(II), 5.89(I)
no Mg^{2+}		6.07(II), 5.88(I)	6.08(II), 5.88(I)

[a] The kinetic data for WT are from Tian et al. (1990), the K_d values for WT from Sanders et al. (1989), and the chemical shift data for WT from Yan et al. (1990a). [b] Determined by monitoring guanidine-HCl-induced unfolding with circular dichroisim (T. Dahnke, unpublished results). The $\Delta G_D^{H_2O}$ and m values were calculated as described in Pace (1986). [c] The sites I and II of the $MgAP_5A$ complexes have been assigned to the AMP and the MgATP sites, respectively (Yan et al., 1990b). [d] This resonance is not resolved, possibly overlapped with the free H_8 (8.42 ppm).

^{31}P NMR Methods. ^{31}P NMR spectra were recorded at 121.496 MHz and 25 °C on a Bruker MSL-300 NMR spectrometer. Samples were in 10-mm NMR tubes and contained 1 mM AK and 1 mM AP_5A in a 75 mM Tris-HCl buffer (pH 8.0) containing 65 mM KCl, 1 mM DTT, 0.5 mM EDTA, 20% ^2H_2O, and the specified concentration of $MgCl_2$. A 70° pulse and a 5-s relaxation delay were used in data acquisition. All spectra were broad-band proton-decoupled with the WALTZ sequence. The spectral width was 40 ppm, and 8K data points were recorded for each spectrum in the quadrature detection mode. A 10-Hz line broadening was applied before Fourier transformation. All chemical shifts were referenced to external 85% H_3PO_4 at 25 °C.

^{25}Mg NMR Methods. ^{25}Mg NMR spectra were acquired at 18.374 MHz without sample spinning on a Bruker MSL-300 spectrometer. The samples were in the same buffer as for ^{31}P NMR experiments. The experiments proceeded by titrating 2.2 mL of 1 mM $^{25}Mg^{2+}$ solution (prepared from the 0.25 M stock solution) with AK (6.3 mM) and/or AP_5A (63 mM) stock solutions. The RIDE pulse sequence was used to reduce the effects of accoustic ringing (Ellis, 1983). The 90° pulse was 30 ms, the spectral width was 2000 Hz, the acquisition time was 256 ms, and the number of transients was 200800. A Lorentzian line broadening of 1 or 15 Hz and two left shifts were applied to the time domain data prior to Fourier transformation.

Results and Discussion

Kinetic Properties of D93A. The steady-state kinetic parameters of D93A, along with those of WT, are listed in Table I. The data were obtained by a full initial velocity analysis varying both substrates (Cleland, 1986). As shown in Table I, replacement of Asp-93 with an alanine residue resulted in virtually no changes in K_i and small increases (ca. 4-fold) in

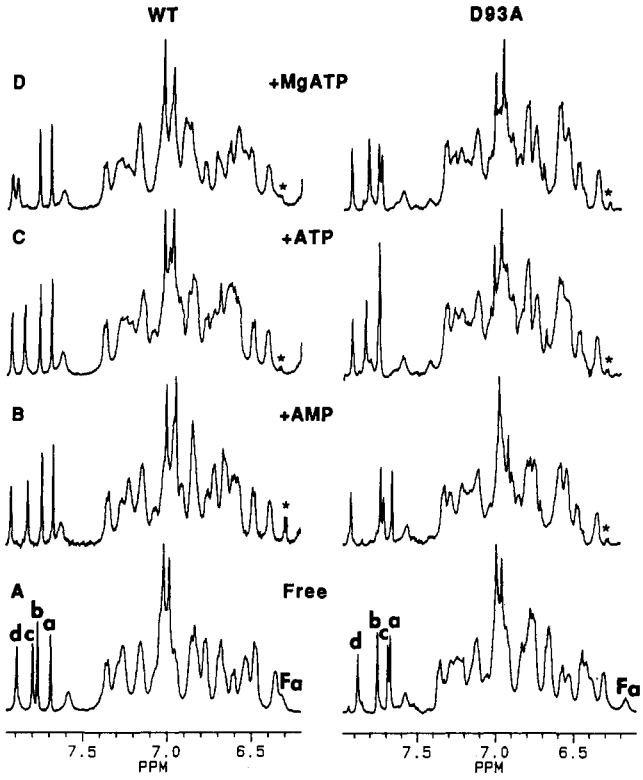

FIGURE 1: One-dimensional proton NMR spectra of the aromatic protons of WT (left panel) and D93A (right panel). The spectra of WT (the left panel) are reproduced from Sanders et al. (1989), except that the spectrum of the AMP complex shown is with larger excess of AMP (ca. 20 mM). The conditions for the right panel are as follows: (A) 0.9 mM D93A; (B) 0.9 mM D93A + 13.5 mM AMP; (C) 1.0 mM D93A + 12.4 mM ATP; (D) 1.5 mM D93A + 12.4 mM ATP + 15.0 mM $MgCl_2$. The FIDs were processes with 1-Hz exponential line broadening. The resonance Fa has been shifted upfield to outside of the spectral range in all complexes. Peaks c and d have been assigned to His-36 and His-30, respectively (Yan et al., 1990a). The sharp doublets at 6.3 ppm, labeled with "*", arise from the ^{13}C satellites of the C1′-H of the excess nucleotides.

K_m but a large decrease in k_{cat} (650-fold). Since the kinetic mechanism of AK is random Bi Bi (Rhoads & Lowenstein, 1968) and the chemical step is nearly rate-limiting for WT (Tian et al., 1990), K_i and K_m are close to the true dissociation constants of the binary and ternary complexes, respectively. As suggested and demonstrated in our previous studies (Yan et al., 1990a,b), it is necessary to perform structural analysis of the mutant enzyme in the free form and in binary and ternary complexes in order to interpret the kinetic data properly.

^1H NMR Analysis of Free D93A. The one-dimensional proton NMR spectra of free D93A and free WT are shown in Figure 1A. Two notable differences are the upfield shifts of the ring C2-H of His-36 (peak c) and the most upfield aromatic resonance (peak Fa). Smaller shifts in other resonances can also be observed. In order to determine whether the chemical shift changes of the two resonances reflect a local structural perturbation or global conformational changes, we performed 2D experiments and assigned the chemical shifts of the aromatic spin systems of D93A in analogy to the previous assignment of WT (Yan et al., 1990a). Analysis of the NOESY spectrum of D93A (Figure 2) indicates that the patterns of the aromatic–aromatic and aromatic–aliphatic interresidue NOEs are similar but not identical to those of WT (Yan et al., 1990a). In the aromatic region the three sets of NOE cross-peaks observed for WT are also present in D93A (peaks a, b, and c in Figure 2). The latter exhibits additional

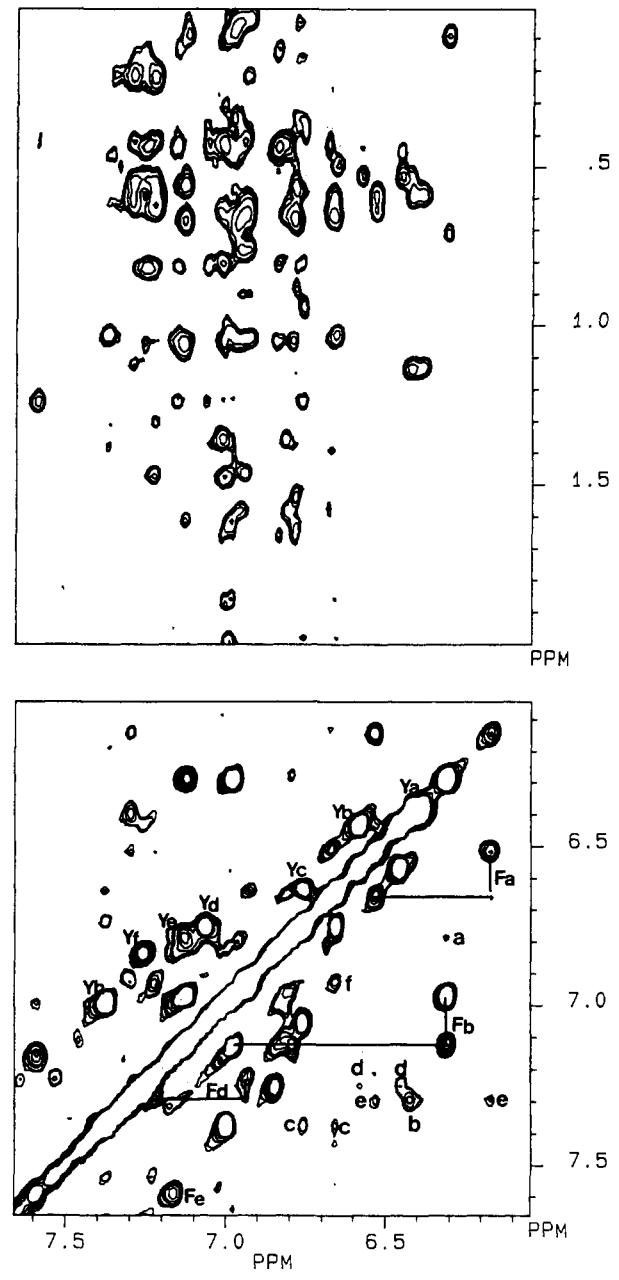

FIGURE 2: NOESY spectrum of free D93A. Cross-peaks a, b, and c have also been observed in WT (Yan et al., 1990a) and can be assigned tentatively to the interresidue NOEs of Fb/Ye, Fd/Ya, and Yc/Yh, respectively. Cross-peaks d, e, and f can be tentatively assigned to Yb/Yf, Fa/Fd, and Fd/Yc, respectively.

NOE cross-peaks, but this does not necessarily suggest a change in conformation since it could be simply due to a better sensitivity in the experiment. Quantitatively, the chemical shifts of the aromatic spin systems of D93A show appreciable changes in only three residues: Fa (6.17, 6.53, and 6.68 ppm, compared to 6.31, 6.51, and 6.62 ppm in WT), Ya (6.38 and 6.42 ppm, compared to 6.41 and 6.49 ppm in WT), and His-36 [7.24 (tentative) and 7.70, compared to 7.20 and 7.78 in WT]. Thus, although there are substantial perturbations in the 1D spectrum of D93A, the effects appear to be largely localized, and the largest change is only −0.14 ppm.

There is no obvious explanation to the relatively large perturbation in Fa, except to say that the aromatic resonances of this residue have been very sensitive to site-specific mutations and to binding of substrates or inhibitors (Sanders et al., 1989; Yan et al., 1990a,b). The perturbation in His-36 is rationalized in the following section.

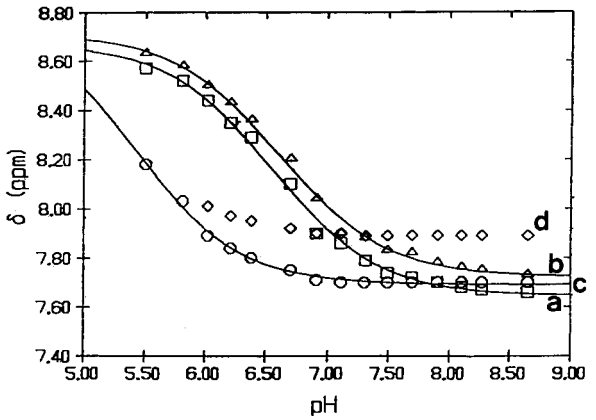

FIGURE 3: Titration curves of the C2-H chemical shifts of the histidine residues in D93A. Curves a–d correspond to His-a, His-b, His-c and His-d, respectively, in Figure 1 and in Yan et al. (1990a) (His-c and His-d correspond to H36 and H30, respectively) but correspond to c, b, a, and d, respectively, in Tian et al. (1988).

Relationship between Asp-93 and His-36. The perturbation in His-36 can be attributed to direct interactions between the carboxylate of Asp-93 and the imidazole ring of His-36: in the 2.1-Å crystal structure of porcine muscle AK (at neutral pH), one of the carboxylate oxygen of Asp-93 (OD1) receives an H-bond from the N3-H of His-36 (Dreusicke et al., 1988). This interpretation is further supported by the perturbation in the pK_a of His-36. Figure 3 shows the nonlinear least-squares fittings of the pH titration data of the histidine residues in D93A. For His-a and His-b, the pK_a values (6.55 and 6.60, respectively) are close to the corresponding values of WT (6.42 for both) and the δ_{H^+} and δ_{H^0} values (chemical shifts of the protonated and unprotonated species, respectively) are essentially unchanged. The pK_a of His-30 (curve d) is also unusually low (not measurable) as in the case of WT. The pK_a of His-36 is normal in WT (6.23) but becomes significantly lower in D93A (<5.5 as estimated from the incomplete curve c in Figure 3), which can be accounted for by stabilization of the positive charge of protonated His-36 by Asp-93 in WT. According to Zimmerman and Cramer (1988), the carboxylate of a syn-oriented Asp–His couple (which appears to be the case for AK on the basis of the crystal structure) can increase the pK_a of the His by as much as 1.5 pH unit.

We have previously shown that substitution of His-36 by Gln, Asn, or Gly resulted in decreases in the conformational stability of AK and suggested that His-36 is involved in conformational stabilization by its interaction with Cys-25 and/or Asp-93 (Tian et al., 1988). In the crystal structure of porcine muscle AK, the same oxygen of Asp-93 (OD1) receiving an H-bond from His-36 is also H-bonded to the thiol group of Cys-25 (Derusicke et al., 1988). Thus one might expect the D93A mutant to be very unstable. However, the data in Table I show that the free energy of unfolding, $\Delta G_D^{H_2O}$, is identical between D93A and WT within experimental errors. This observation is quite unexpected and suggests that the instability of His-36 mutants is likely to be due to exposure of the thiol group of Cys-25 rather than disruption of the interaction between His-36 and Asp-93.

^1H NMR Analysis of Binary Complexes. In order to assess the effects of substituting Asp-93 with Ala and the accompanying perturbations in H36 and Fa on the binding of substrates, titration experiments were performed by monitoring the ^1H chemical shifts of AK while varying the concentrations of AMP, ATP, or MgATP. The spectra of the final points of titration are shown in Figure 1 (B, C, and D, respectively). The dissociation constants K_d obtained by nonlinear least squares fitting of the titration data are listed in Table I, and representative fitting curves are shown in Figure 4. As shown by the data in Table I, the K_d values of the binary complexes of D93A are close to the corresponding values of WT, which agrees with the lack of perturbation in the K_i values obtained from steady-state kinetics.

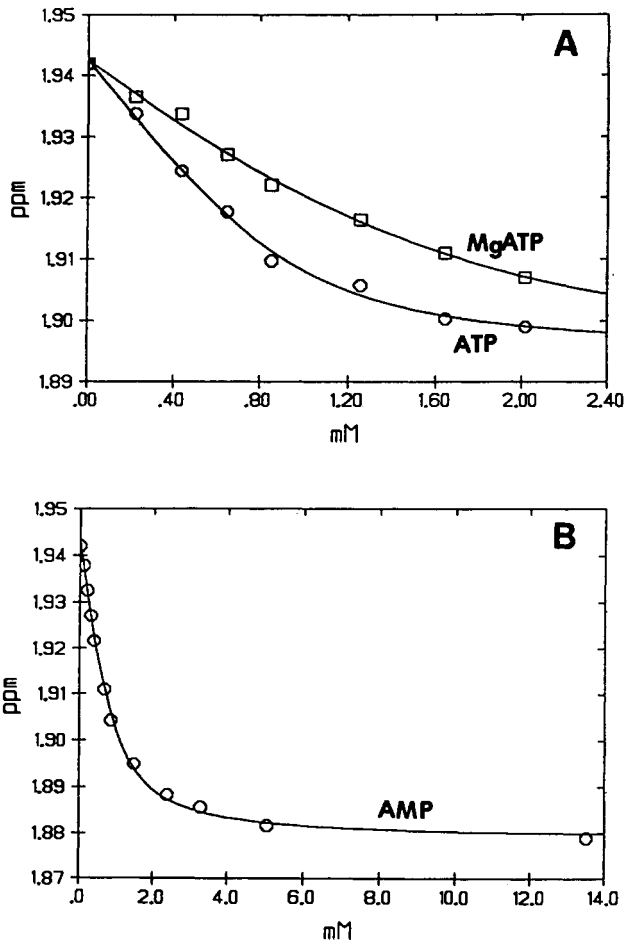

FIGURE 4: Chemical shift curves from titrations of D93A with MgATP and ATP (A) and AMP (B). Solid lines represent 1:1 nonlinear least-squares fittings of the titration data. The chemical shifts on the *y*-axes are those of the most upfield CH_3 resonance of methionines.

The chemical shifts of the adenine H_2, H_8, and adenosine $H_{1'}$ protons of bound nucleotides have been deduced from the titration studies. The differences between the chemical shifts of the nucleotides bound to WT (Yan et al., 1990a) and D93A are ≤0.1 ppm for all binary complexes. Thus both dissociation constants and chemical shifts of bound nucleotides suggest that the binary complexes of D93A have very similar properties relative to the corresponding binary complexes of WT. However, careful examination of the 1D spectra revealed substantial differences, particularly between WT+AMP and D93A+AMP (Figure 1B). Since perturbations in the ternary complex is even more extensive, we proceeded to analyze the ternary complex in detail as described in the next section.

^1H NMR Analysis of the D93A+$MgAp_5A$ Complex. The ternary complex was characterized by use of a bisubstrate analogue, $MgAP_5A$, and the 1D proton NMR spectra are shown in Figure 5 (A and C). Since appreciable differences exist between the 1D spectra of WT+$MgAP_5A$ and D93A+$MgAP_5A$, we pursued quantitative (or semi-quantitative) comparison using NOESY spectra and aromatic spin systems.

The aromatic spin systems, assigned from 1D and NOESY spectra and from comparison with the previous assignments of WT+$MgAP_5A$ (Yan et al., 1990a), show appreciable

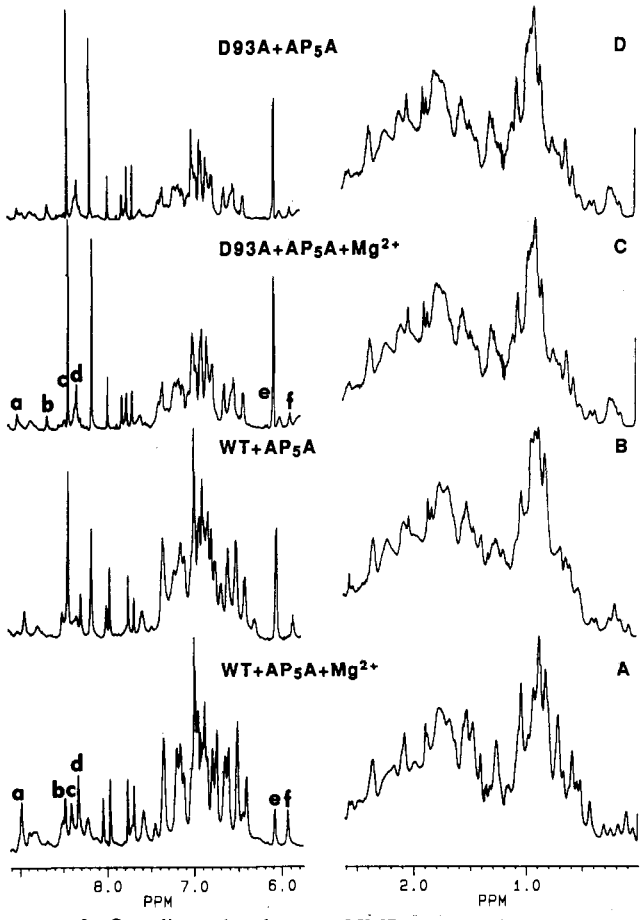

FIGURE 5: One-dimensional proton NMR spectra of various AP_5A complexes: (A) 2.5 mM WT + 2.5 mM AP_5A + 5.0 mM $MgCl_2$; (B) 2.0 mM WT + 4.0 mM AP_5A; (C) 1.7 mM D93A + 4 mM AP_5A + 5 mM $MgCl_2$; (D) 1.7 mM D93A + 4 mM AP_5A. The FIDs were processed with Guassian multiplication (LB = −5, GB = 0.1). Spectra A and B are reproduced from Yan et al. (1990a). Peaks a–f are due to bound $MgAP_5A$: a, H_2(I); b, H_8(I); c, H_8(II); d, H_2(II); e, $H_{1'}$(II); f, $H_{1'}$(I). The three sharp and intense resonances in spectra B–D arise from excess AP_5A.

perturbations in only four residues: Fa (5.99, 6.55, and 6.76 ppm, which are shifted by −0.45, +0.04, and +0.11 ppm, respectively), Xb (6.89 and 7.20, shifted by −0.08 ppm for the first resonance), Ye (6.82 and 7.10, shifted by −0.06 ppm for the first resonance), and H36 (7.80 for H_2, shifted by −0.24 ppm; unresolved for H_4). These data suggest that while the perturbations in the chemical shifts of Fa and His-36 become more significant (relative to the perturbations in the free enzyme), the changes in other resonances are minimal. Analysis of the NOESY spectrum of D93A+$MgAP_5A$ (not shown) suggests that it retains the three major sets of the aromatic–aromatic interresidue NOEs observed in the WT+$MgAP_5A$ complex (cross-peaks p, q, and r in the Figure 6 of Yan et al., 1990a) and that the NOE patterns in the aromatic–aliphatic regions are qualitatively similar between the WT and the mutant complexes. These results taken together suggest that the two complexes have similar conformations and that the structural perturbation in the $MgAP_5A$ complex (as a static mimic of the ternary complex) is also localized. Thus the large decrease in k_{cat} can be attributed to stabilization of the transition state by the carboxylate of Asp-93, by ca. 3.9 kcal/mol.

The chemical shifts of the adenine H_2, H_8, and adenosine $H_{1'}$ protons of bound AP_5A have also been assigned and listed in Table I. There are notable differences (0.18 ppm in the presence of Mg^{2+}, 0.15 ppm in the absence of Mg^{2+}) between D93A and WT in the H_8 resonances of the adenosine I (at the AMP site, Yan et al., 1990b). The significance of such differences is unclear.

Asp-93 Mediates the Binding of Mg^{2+}. After demonstrating the catalytic significance of Asp-93 by kinetic and ^1H NMR studies, the question of *how* Asp-93 participates in catalysis follows. Careful examination of the 1D proton NMR spectra revealed that the spectra of D93A+ATP (Figure 1C) and D93A+MgATP (Figure 1D) are very similar and that the spectra of D93A+AP_5A (Figure 5D) and D93A+$MgAP_5A$ (Figure 5C) are essentially identical. These are in contrast to the case of WT, where notable differences exist between the complexes with and without Mg^{2+}, particularly in the region of 6.4–6.8 ppm for WT+ATP (Figure 1C) and WT+MgATP (Figure 1D) and the regions of 6.3–6.8 ppm and 0.5–2.1 ppm for WT+AP_5A (Figure 5B) and WT+$MgAP_5A$ (Figure 5A). The chemical shifts of bound AP_5A listed in Table I also indicate nearly identical values between D93A+AP_5A and D93A+$MgAP_5A$ but detectable differences between WT+AP_5A and WT+$MgAP_5A$. These results suggest that Asp-93 is interacting (possibly directly) with the bound Mg^{2+} ion in the AK+$MgAP_5A$ complex. This interpretation is consistent with the crystallographic observation that Asp-93 is close to the bound Mg^{2+} ion in the yeast AK·$MgAP_5A$ complex (Egner et al., 1987).

The next question, then, is whether (and how) disruption of the interaction between Mg^{2+} and Asp-93 affects binding of Mg^{2+} to the phosphate groups of AP_5A. This question was probed by examining the effects of Mg^{2+} on the ^{31}P NMR signals of AP_5A bound to WT and D93A, as shown in Figure 6. The results for WT are very similar to those of porcine muscle AK reported previously (Nageswara Rao & Cohn, 1977): in the absence of Mg^{2+} ions, the NMR spectrum reveals two groups of resonances (at −10.8 and −11.7 and at −21.6, −22.3, and −23.5 ppm); upon addition of Mg^{2+} ions, all five resonances become distinct and well resolved (at −10.4, −12.2, −18.5, −22.7, and −25.1 ppm). The spectrum of D93A+AP_5A is similar to that of WT+AP_5A (−10.9, −11.1, −20.6, −21.4, and −23.8 ppm). However, addition of Mg^{2+} ions to the D93A+AP_5A solution caused virtually no changes in the NMR spectrum. This is surprising since even in the absence of AK, Mg^{2+} induces ca. 1 ppm shifts in the ^{31}P resonances of AP_5A (spectra not shown; also Nageswara Rao & Cohn, 1977).

The large differences in chemical shifts in the WT+$MgAP_5A$ complex relative to the WT+AP_5A complex could be due to asymmetric binding of the Mg^{2+} ion and the resultant conformational changes in the polyphosphate chain of AP_5A. The inability of Mg^{2+} ions to induce changes in the spectrum of the D93A+AP_5A complex suggests that Asp-93 is required for proper interaction of Mg^{2+} with the phosphate groups.

Can Mg^{2+} Bind to the D93A·AP_5A Complex? The observation that Mg^{2+} ions do not induce any detectable change in either ^1H or ^{31}P NMR spectra of D93A+AP_5A led us to suspect whether Mg^{2+} ions can bind to the complex at all, even though there is no obvious reason that the binding of Mg^{2+} ions with AP_5A at the active site should be prohibited by substituting Asp-93 with Ala. This problem was probed by ^{25}Mg NMR, and the spectra are shown in Figure 7. The ^{25}Mg nucleus is quadrupolar with $I = 5/2$, and the detailed theories in using ^{25}Mg NMR to study Mg^{2+} binding to proteins are quite complicated as described previously (Tsai et al., 1987; Sanders & Tsai, 1989). In short, the line width ($\Delta\nu$) is determined by a number of factors: exchange rate, binding constant, relaxation times, quadrupolar coupling constants, and rotational correlation times (of both free and bound forms

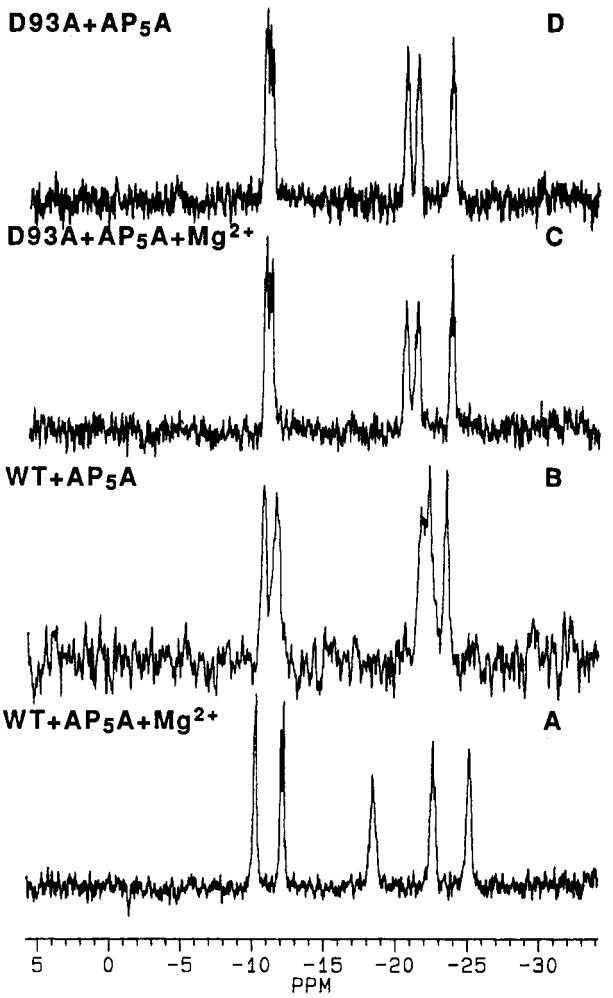

FIGURE 6: ^{31}P NMR spectra of various AP_5A complexes: (A) 1 mM WT + 1 mM AP_5A + 2 mM $MgCl_2$; (B) 1 mM WT + 1 mM AP_5A; (C) 1 mM D93A + 1 mM AP_5A + 2 mM $MgCl_2$; (D) 1 mM D93A + 1 mM AP_5A. Spectrum C remained unchanged upon further addition of 2 mM $MgCl_2$.

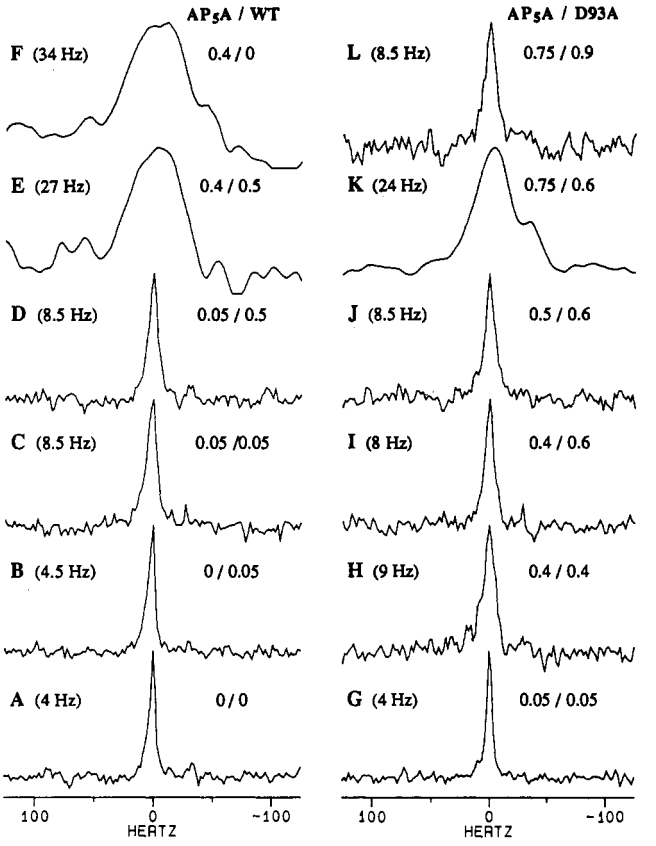

FIGURE 7: ^{25}Mg NMR spectra of 1 mM Mg^{2+} titrated with AP_5A/WT (left panel) and with AP_5A/D93A (right panel). The concentrations (in mM) of AP_5A/WT or D93A/AP_5A are indicated in each spectrum. The FIDs were processed with 1-Hz exponential multiplication except E, F, and K, which were processed with 15 Hz. The numbers in parentheses are the line widths obtained from line fitting and after correcting for the artificial line broadening.

for the latter three factors). The system of AK does not permit complete analysis due to limited stability of the enzyme. However, useful information can be obtained by comparing the behavior of WT and D93A, as described below.

Comparisons between spectra A and B, and between spectra C and D of Figure 7, indicate that addition of the enzyme causes no changes in the line width of the signal within experimental errors. This confirms that the free AK does not bind Mg^{2+} and also ensures that the viscosity change due to addition of AK does not induce any appreciable line broadening under our experimental conditions. Comparisons between spectra B and C, and between spectra D and E, indicate that the ^{25}Mg signal is broadened significantly upon binding to WT+AP_5A. Comparison between spectra E and F suggests that the overall line-broadening effect is similar between WT+AP_5A and free AP_5A, which is unusual but not unreasonable since the line width is dependent on several factors as mentioned earlier. With these information in place, we can then examine the behavior of D93A (spectra G to L). Comparison between spectra A and G indicates that 5% of D93A+AP_5A has virtually no detectable effect on the line width of Mg^{2+}, which is apparently different from the case of WT where the $\Delta\nu$ is doubled under the same condition (spectrum C). However, comparison of spectrum A with spectra H, I, and J suggests that the signal is indeed broadened (the $\Delta\nu$ is doubled) by 40–50% of D93A+AP_5A. The excessive broadening in spectrum K is due to the excess AP_5A, as indicated by the sharpening of signal in spectrum L upon addition of more enzyme to sample K. These results suggest that Mg^{2+} ions do bind to the D93A+AP_5A complex, but the binding results in substantially smaller degree of line broadening. If both systems are under the fast exchange and exchange narrowing conditions (which are the most likely conditions judging from all factors), the smaller extent of line broadening in D93A could be due to the combination of several factors: lower affinity, higher rotational freedom, and smaller quadrupolar coupling constant, all of which could result from the lack of coordination between Mg^{2+} and Asp-93. If the WT system is in slow or intermediate exchange, the small extent of line broadening in D93A could be due to increased exchange rates in the D93A system, which is also consistent with weaker binding (lower affinity).

Can the Activity of D93A Be Restored by Higher [Mg^{2+}]? Since the result of ^{25}Mg NMR suggests a lower affinity of Mg^{2+} ions toward the D93A+AP_5A complex, one may ask whether the activity of D93A can be restored by higher concentrations of Mg^{2+} ions. There was a physical evidence against such a possibility: as stated in the legend of Figure 6, further addition of Mg^{2+} to the spectrum C of Figure 6 did not induce any obvious change. To provide further support to the physical studies, we determined the specific activities of WT and D93A as a function of [Mg^{2+}]. As shown in Figure 8, the activity of WT reaches maximum at 1 mM [Mg^{2+}] and then decreases to a ca. 50% level. Such a behavior has been well known for AK (Noda, 1958), but the exact nature is not fully understood. For D93A, there appears to be no "Mg^{2+} inhibition", and the reason is again unclear. However, it is

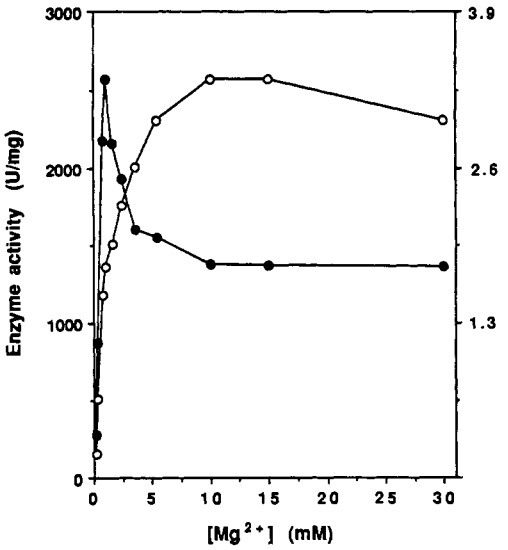

FIGURE 8: Specific activities of WT (closed circles, left y-axis) and D93A (open circles, right y-axis) as a function of [Mg^{2+}]. The experiments were performed under our normal assay condition, with ATP and AMP held at 1 and 2 mM, respectively.

quite obvious that *excess Mg^{2+} ions cannot restore the activity of D93A*. The smaller increases in the beginning part of the titration curve for D93A (relative to that of WT) also supports lower affinity of Mg^{2+} toward the D93A+ nucleotide complex.

The Roles of Asp-93 and Mg^{2+} Ions in Catalysis. All of our results suggest that removal of the carboxylate of D93A causes a modest decrease in the affinity of Mg^{2+} and a large decrease in k_{cat}, but the former is not the direct cause of the latter. The decrease in binding affinity is consistent with the involvement of Asp-93 in the binding of Mg^{2+} (when ATP or AP_5A is also bound). The decrease in k_{cat} should be due to an increase in the free energy level of the transition state, which is further elaborated as follows.

Mg^{2+} ions could play both chemical and structural roles in the catalysis by kinases. The possible chemical roles are to shield the charge of the γ-phosphoryl group from the attacking nucleophile, and to enhance the cleavage of the P_γ–O bond by electrophilic effects. The structural role is to orient the phosphate chains in proper conformation. The ^{31}P NMR results specifically suggest that in the absence of the carboxylate of Asp-93 the Mg^{2+} ion is unable to orient the phosphate chain of bound AP_5A. Thus, Asp-93 is required for fixing the Mg^{2+} ion at the proper position, which in turn leads to proper orientation of the phosphate groups. The structural role of Mg^{2+} is clearly impaired in D93A. Since D93A still achieves a rate enhancement of ca. 10^9 and the reaction still requires Mg^{2+} ions, the chemical roles of Mg^{2+} ions may not have been greatly impaired in the catalysis by D93A.

An interesting and important question to ask is *when* does Mg^{2+} come into play during the catalytic cycle. The results from previous studies and the present ^{25}Mg NMR experiments clearly show that free AK does not bind Mg^{2+} ions. Whether Asp-93 interacts with Mg^{2+} in the binary complex with MgATP has not been explicitly addressed. However, the fact that AK binds uncomplexed ATP with 4-fold higher affinity than MgATP (Sanders et al., 1989) but it shows higher affinity to $MgAP_5A$ than to uncomplexed AP_5A (Reinstein et al., 1990) suggests that the function of Asp-93 in binding the Mg^{2+} ion is more significant in the ternary complex than the binary complex. Thus, the interaction between AK and the bound Mg^{2+} ion is more important at the later stage of the catalytic cycle and is possibly most important at the transition state. Such interpretations can explain the previous observations that AK can bind different metal·ATP complexes nonproductively but is fairly specific to MgATP in catalysis (Dunaway-Mariano & Cleland, 1980; Cohn, 1982). However, the interaction between Mg^{2+} and Asp-93 at the transition state is not an absolute requirement and accounts for only ca. 3.9 kcal/mol.

Using time-resolved X-ray crystallography, Schlichting et al. (1990) have observed that in the complex between the *ras* p21 protein and MgGTP, the Mg^{2+} ion is coordinated to the β- and γ-phosphate groups of the nucleotide and interacts with Asp-57 through a water bridge. In the p21+MgGDP complex, the Mg^{2+} ion accepts only one ligand from the nucleotide (the β-phosphoryl group) but is coordinated directly to Asp-57. On the basis of the paramagnetic effects on the ^{31}P NMR relaxation rates of bound nucleotides, Ray et al. (1988) have also shown that in porcine muscle AK the metal ion Co^{2+} is within first coordination sphere distances to the β-phosphate and γ-phosphate of bound CoATP or CoGTP and to the β-phosphate of bound CoGDP. Although Mg^{2+} also interacts with residues other than Asp-57 in the p21 protein, which could be different in the case of AK, it is possible that Mg^{2+} may function in a similar mechanism in the two proteins, with the Asp-93 of AK corresponding to the Asp-57 of the *ras* p21 protein. It will be interesting to see whether the functional relationship between Mg^{2+} and Asp-93 as demonstrated for AK can also be demonstrated in the *ras* p21 protein.

ACKNOWLEDGMENTS

We are indebted to Dr. J. Markley for hosting us at the National Magnetic Resonance Facility at Madison, to Dr. A. Nakazawa for providing us the original *E. coli* strain carrying the WT cAK gene, to Dr. J. Cowan for the generous gift of the $^{25}Mg^{2+}$ stock solution and for assistance in setting up ^{25}Mg NMR experiments, to T. Dahnke for measuring $\Delta G_D^{H_2O}$, and to Y. Li for purifying part of the D93A AK.

REFERENCES

Cleland, W. W. (1986) in *Investigation of Rates and Mechanisms of Reactions Part 1* (Bernasconi, C. F., Ed.), pp 791–870, Wiley, New York.

Cohn, M. (1982) *Acc. Chem. Res. 15*, 326–332.

Dreusicke, D., Karplus, P. A., & Schulz, G. (1988) *J. Mol. Biol. 199*, 359–371.

Dunaway-Mariano, D., & Cleland, W. W. (1980) *Biochemistry 19*, 1506–1515.

Egner, U., Tomasselli, A. G., & Schulz, G. E. (1987) *J. Mol. Biol. 195*, 649–658.

Ellis, P. D. (1983) in *The Multinuclear Approach to NMR Spectroscopy* (Lambert, J. B., & Riddell, F. G., Eds.) pp 425–523, Reidel, Boston, MA.

Fry, D. C., Kuby, S. A., & Mildvan, A. S. (1985) *Biochemistry 24*, 4680–4694.

Gorenstein, D. (1989) *Methods Enzymol. 177*, 295–316.

Kim, H. J., Nishikawa, S., Tokutomi, Y., Takenaka, H., Hamada, M., Kuby, S. A., & Uesugi, S. (1990) *Biochemistry 29*, 1107–1111.

Kishi, F., Maruyama, M., Tanazawa, Y., & Nakazawa, A. (1986) *J. Biol. Chem. 261*, 2942–2945.

Markley, J. L. (1974) *Acc. Chem. Res. 8*, 70–80.

McDonald, G. G., Cohn, M., & Noda, L. H. (1975) *J. Biol. Chem. 250*, 6947–6954.

Mildvan, A. S. (1979) *Adv. Enzymol. Relat. Areas Mol. Biol. 49*, 103–126.

Mildvan, A. S., & Cohn, M. (1970) *Adv. Enzymol. Relat. Areas Mol. Biol. 33*, 1–70.

Mildvan, A. S., & Fry, D. C. (1987) *Adv. Enzymol. Relat. Areas Mol. Biol. 58*, 241–313.

Nageswara Rao, B. D., & Cohn, M. (1977) *Proc. Natl. Acad. Sci. U.S.A. 74*, 5355-5357.
Noda, L. (1958) *J. Biol. Chem. 232*, 237-250.
Pace, C. N. (1986) *Methods Enzymol. 131*, 266-280.
Ray, B. D., Rösch, P., & Nageswara Rao, B. D. (1988) *Biochemistry 27*, 8669-8676.
Reinstein, J., Vetter, I. R., Schlichting, I., Rösch, P., Wittinghofer, A., & Goody, R. (1990) *Biochemistry 29*, 7440-7450.
Rhoads, D. G., & Lowenstein, J. M. (1986) *J. Biol. Chem. 243*, 3963-3972.
Sanders, C. R., II, Tian, G., & Tsai, M.-D. (1989) *Biochemistry 28*, 9028-9043.
Sanders, C. R., II, & Tsai, M.-D. (1989) *Methods Enzymol. 177*, 317-333.
Schlichting, I., Almo, S. C., Rapp, G., Wilson, K., Petratos, K., Lentfer, A., Wittinghofer, A., Kabsch, W., Pai, E. F., Petsko, G. A., & Goody, R. S. (1990) *Nature 345*, 309-315.
Schulz, G. E. (1987) *Cold Spring Harbor Symp. Quant. Biol. 52*, 429-439.
Smith, G. M., & Mildvan, A. S. (1982) *Biochemistry 21*, 6119-6123.
Tanizawa, Y., Kishi, F., Kaneko, T., & Nakazawa, A. (1987) *J. Biochem. (Tokyo) 101*, 1289-1296.
Taylor, J. W., Schmidt, W., Cosstick, R., Okruszek, A., & Eckstein, F. (1985a) *Nucleic Acid Res. 13*, 8749-8764.
Taylor, J. W., Ott, J., & Ecstein, F. (1985b) *Nucleic Acid Res. 13*, 8764-8785.
Tian, G., Sanders, C. R., II, Kishi, F., Nakazawa, A., & Tsai, M.-D. (1988) *Biochemistry 27*, 5544-5552.
Tian, G., Yan, H., Jiang, R.-T., Kishi, F., Nakazawa, A., & Tsai, M.-D. (1990) *Biochemistry 29*, 4296-4304.
Tsai, M.-D., Drakenberg, T., Thulin, E., & Forsén, S. (1987) *Biochemistry 26*, 3635-3643.
Yan, H., Shi, Z., & Tsai, M.-D. (1990a) *Biochemistry 29*, 6385-6392.
Yan, H., Dahnke, T., Zhou, B., Nakazawa, A., & Tsai, M.-D. (1990b) *Biochemistry 29*, 10956-10964.
Zimmerman, S. C., & Cramer, K. D. (1988) *J. Am. Chem. Soc. 110*, 5906-5908.

Laser Flash Photolysis Studies of the Kinetics of Electron-Transfer Reactions of *Saccharomyces* Flavocytochrome b_2: Evidence for Conformational Gating of Intramolecular Electron Transfer Induced by Pyruvate Binding†

Mark C. Walker‡ and Gordon Tollin*
Department of Biochemistry, University of Arizona, Tucson, Arizona 85721
Received August 23, 1990; Revised Manuscript Received March 5, 1991

ABSTRACT: The kinetics of reduction of the flavocytochrome from *Saccharomyces cerevisiae* by exogenous deazaflavin semiquinones have been investigated by using laser flash photolysis. Direct reduction by deazaflavin semiquinone of both the b_2 heme and the FMN cofactor occurred via second-order kinetics with similar rate constants (9×10^8 M^{-1} s^{-1}). A slower, monoexponential, phase of FMN reoxidation was also observed, concurrent with a slow phase of heme reduction. The latter accounted for approximately 20–25% of the total heme absorbance change. Both of these slow phases were protein concentration dependent, yielding indentical second-order rate constants (1.1×10^7 M^{-1} s^{-1}), and were interpreted as resulting from intermolecular electron transfer from the FMN semiquinone on one protein molecule to an oxidized heme on a second molecule. Consistent with this conclusion, no slow phase of heme reduction was observed with deflavo-flavocytochrome b_2. Upon the addition of pyruvate (but not D-lactate or oxalate), the second-order rate constant for heme reduction was unaffected, but direct reduction of the FMN cofactor was no longer observed. Reduction of the heme cofactor was followed by a slower partial reoxidation, which occurred concomitantly with a monoexponential phase of FMN reduction. Both processes were protein concentration independent and were interpreted as the result of intramolecular electron transfer from reduced b_2 heme to oxidized FMN. Potentiometric titrations of the flavocytochrome in the absence and presence of pyruvate demonstrated that the thermodynamic driving force for electron transfer from FMN to heme is much greater in the absence of pyruvate. Despite this, intramolecular electron transfer was only observed in the presence of pyruvate. This result is interpreted in terms of a conformational change induced by pyruvate binding which permits electron transfer between the cofactors. The rate constant for intramolecular electron transfer in the presence of pyruvate was dependent on ionic strength, suggesting the occurrence of electrostatic effects which influence this process.

Yeast flavocytochrome b_2 (L-lactate dehydrogenase, EC 1.1.2.3) is a bifunctional enzyme (Jacq & Lederer, 1974) that catalyzes the two-electron oxidation of L-lactate to pyruvate, and subsequent one-electron transfers to two cytochrome *c* molecules (Labeyrie et al., 1978; Capeillere-Blandin et al., 1980; Labeyrie, 1982). The protein exists in solution as a tetrameric assembly of monomers, each with a molecular weight of 57 500. The crystal structure for the enzyme from *Saccharomyces cerevisiae* has been determined at 2.4-Å resolution (Xia et al., 1987; Mathews & Xia, 1987; Xia & Mathews, 1990) and demonstrates that the monomer is folded into two functionally distinct domains. The flavodehydrogenase domain contains the FMN[1] cofactor, substrate

† This work was supported in part by Grant DK15057 from the National Institutes of Health (to G.T.).
* To whom correspondence should be addressed.
‡ Present address: Monsanto Agricultural Co., 800 N. Lindbergh Blvd., St Louis, MO 63167.

0006-2960/91/0430-5546$02.50/0